

# Paleoceanography and Paleoclimatology



## RESEARCH ARTICLE

10.1029/2021PA004299

### Key Points:

- Ostracod assemblages evidenced relative regional sea-level variations likely linked to glacioeustasy related to global climate fluctuations
- Clumped isotopes show large temperature and salinity variations in the Hampshire basin during middle Eocene
- Sea-level variations and high-latitude water mixing ruled by the English Channel gateway influenced regional temperature and salinity

### Correspondence to:

M. Marchegiano,  
[marta.marchegiano@vub.be](mailto:marta.marchegiano@vub.be)

### Citation:

Marchegiano, M., & John, C. M. (2022). Disentangling the impact of global and regional climate changes during the middle Eocene in the Hampshire Basin: New insights from carbonate clumped isotopes and ostracod assemblages. *Paleoceanography and Paleoclimatology*, 37, e2021PA004299. <https://doi.org/10.1029/2021PA004299>

Received 3 MAY 2021  
 Accepted 20 JAN 2022

### Author Contributions:

**Conceptualization:** Marta Marchegiano  
**Formal analysis:** Marta Marchegiano  
**Funding acquisition:** Marta Marchegiano, Cédric M. John  
**Investigation:** Marta Marchegiano  
**Methodology:** Marta Marchegiano  
**Resources:** Cédric M. John  
**Supervision:** Cédric M. John  
**Validation:** Cédric M. John  
**Writing – original draft:** Marta Marchegiano, Cédric M. John  
**Writing – review & editing:** Marta Marchegiano, Cédric M. John

© 2022. The Authors.

This is an open access article under the terms of the [Creative Commons Attribution License](https://creativecommons.org/licenses/by/4.0/), which permits use, distribution and reproduction in any medium, provided the original work is properly cited.

## Disentangling the Impact of Global and Regional Climate Changes During the Middle Eocene in the Hampshire Basin: New Insights From Carbonate Clumped Isotopes and Ostracod Assemblages

Marta Marchegiano<sup>1,2</sup>  and Cédric M. John<sup>1</sup>

<sup>1</sup>Department of Earth Science & Engineering, Imperial College London, London, UK, <sup>2</sup>Now at Research unit: Analytical, Environmental and GeoChemistry, Vrije Universiteit Brussel, Brussel, Belgium

**Abstract** We present a novel multiproxy data set (bulk and clumped isotopes on gastropod shells and variations in ostracod assemblages) of the Hampshire Basin (Southern-England) that sheds light on the connection between the North Sea and the Atlantic Ocean through the English Channel during the deposition of the Barton clay formation (latest Lutetian—Bartonian, middle Eocene; ~41–40 Ma). During this time period, the English Channel operated as a gateway between the warmer Atlantic Ocean and the colder North Sea waters. High-latitude water mixing combined with the regional hydrological cycle and sea-level variations, may have contributed to mitigate the water temperatures in the Hampshire Basin, with an average recorded of ca. 25°C. In the uppermost part of the section the connection between the two water masses was limited or absent as evidenced by warmer (up to ca. 35°C) Atlantic Ocean temperatures in the Hampshire Basin. The large differences in average oxygen isotope composition of seawater ( $\delta^{18}\text{O}_{\text{water}}$ ) recorded (from  $\delta^{18}\text{O}_{\text{water}} - 1.7\text{‰}$  to  $\delta^{18}\text{O}_{\text{water}}$  of  $-0.7\text{‰}$ ) evidenced large salinity differences between the Atlantic Ocean and the North Sea. Ostracods suggest that the temporary connection between those two water masses was caused by relative regional sea-level variations. This scenario could be partially linked to glacio-eustatic sea-level changes related to climate fluctuations probably associated with the MECO event.

## 1. Introduction

In 2013 the IPCC (Stocker et al., 2013) estimated up to 5°C global warming by 2100 associated with the rapid rise of anthropogenic atmospheric CO<sub>2</sub>. Coastal and shelf seas play an important role in the uptake of atmospheric CO<sub>2</sub> through a process known as the “continental shelf pump” (Thomas, 2004). Increased export productivity of continental shelves leads to the subtraction of CO<sub>2</sub> from the atmosphere and carbon sequestration in sediments at geological timescales (John et al., 2008). Precise evaluation of the effects of regional climate changes is therefore essential to accurately forecast climate scenarios as well as the ecological response of distinct geographic areas in a warmer world.

Starting from the middle Eocene, the Earth entered a cooling phase that slowly brought the climate from a “greenhouse” to a “icehouse” state at the Eocene-Oligocene boundary. This broad climatic trend was interrupted by a short (~500 ka) globally recorded warm event called Middle Eocene Climatic Optimum (MECO; ~40 Ma) (Bohaty et al., 2009; Bohaty & Zachos, 2003) a potential deep-time analogue for current warming. During MECO, an increase of about 4–6°C of surface and deep sea water is interpreted based on the oxygen isotope composition of benthic foraminifers ( $\delta^{18}\text{O}_{\text{carbonate}}$ ) from deep-sea cores (Bohaty et al., 2009; Bohaty & Zachos, 2003).

The main recorded effects of the MECO in open, deep and large marine basins are the shallowing of the lysocline and the carbonate compensation depth (CCD) as evidenced by a global carbonate decrease caused by seawater acidification (Bohaty et al., 2009) and the reduced amount of nutrients and oxygenation in the sea-floor (Boscolo Galazzo et al., 2015; Cramwinckel et al., 2019). Although no species extinction has been recorded, significant biotic changes have been documented during the MECO (Boscolo Galazzo et al., 2015; Cramwinckel et al., 2019; Rivero-Cuesta et al., 2019; Toffanin et al., 2011).

Middle Eocene paleoclimatic reconstructions and the consequences of the MECO on restricted hemipelagic basins were only recently evidenced at the Baskil section (Turkey), part of the Neo-Tethys (Giorgioni et al., 2019) and by Cramwinckel et al. (2020) in the Labrador Sea. The effects of middle Eocene climatic changes and of

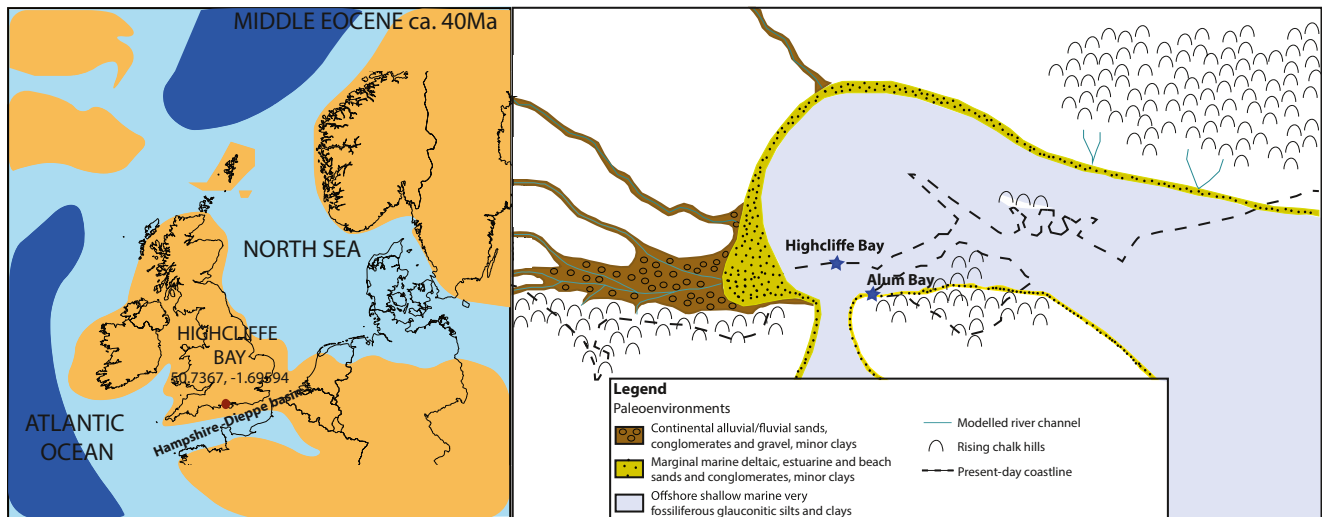


**Figure 1.** (a) Paleogeographical position of the Highcliffe Bay section (red dot) during the middle Eocene (based on Scotese 2016). (b) Depositional environments and paleoceanography of the Hampshire Basin during the deposition of the Barton Clay formation (modified from Barnet, 2021).

global warming events such as the MECO on coastal and shelf seas are thus understudied. Researching this topic is important because these carbon sinks play an important role in regulating global climate and ocean circulations.

Shelf seas and semi-enclosed basins are more challenging to study. Numerical simulations of past hothouse periods (Zhu et al., 2020) have revealed the existence of potentially different water masses with distinct oxygen isotope compositions ( $\delta^{18}\text{O}_{\text{water}}$ ) and regional differences depending on latitude and a number of other factors (e.g., ocean circulation and the hydrological cycle). Reconstruction of past temperatures in coastal environments using oxygen isotopes is more complicated since changes in  $\delta^{18}\text{O}_{\text{water}}$  induce a bias in calculated temperatures ( $\sim\pm 5^\circ\text{C}$  per ‰ units change; Zhu et al., 2020).

This study presents the first record of clumped isotopes ( $\Delta_{47}$ ) and bulk isotopes ( $\delta^{18}\text{O}$  and  $\delta^{13}\text{C}$ ) from well-preserved, aragonitic gastropods shells of the middle Eocene Barton Clay Formation (latest Lutetian—Bartonian, middle Eocene;  $\sim 41$ – $40$  Ma, Hampshire Basin, Barton-on-Sea, UK), a section that possibly records the MECO event (Figure 1). The section at Barton-on-Sea is considered to be one of the best-preserved Paleogene sequences worldwide as the rich and pristine fossil content allows for unbiased paleoclimate and paleoenvironment reconstructions, something extremely rare in Paleogene sequences. The International Subcommission on Palaeogene Stratigraphy (ISPS) designated the Barton Clay Formation in the Hampshire Basin, south UK, as a target to establish the Bartonian chronostratigraphy and the succession between Highcliffe and Barton-on-Sea is the unit stratotype (Cotton et al., 2021). However, because of the poor preservation of the outcrop due to cliff collapses (Barton & Pearce, 2015), investigations to define a Global Stratotype Section and Point (GSSP) for the base of the Bartonian have focused on other areas, and major improvements in the age model as well as in the biostratigraphy of the Barton Clay has been made at the parastratotype section at Alum Bay (7 km away from the Highcliffe section, Figure 1).

The Hampshire Basin represents the north westerly component of the larger Anglo-Paris-Belgium Basin. Central to the motivation for our study is that the Hampshire Basin is located at a critical juncture between the North Sea and the Atlantic Ocean (Figure 1). The North Sea is a highly productive shelf sea where  $\text{CO}_2$  pumping is largely controlled by the exchange of water masses with the North Atlantic Ocean (Salt et al., 2013). During middle-late Eocene, the seaway corresponding to the modern English Channel constituted an important physical boundary between colder and less saline North Sea waters (with more negative estimated oxygen isotope compositions ( $\delta^{18}\text{O}_{\text{water}}$ )) and warmer and more saline North Atlantic waters (with more positive estimated  $\delta^{18}\text{O}_{\text{water}}$ ; Zhu et al., 2020; Figure 1). Moreover, evidence suggests that the connection between the North Atlantic Ocean and the North Sea influenced Northern Europe climatic patterns since at least the late Eocene (Śliwińska et al., 2019).

The overall goal of our study is to assess the degree of connectivity between the North Sea and North Atlantic waters during the middle Eocene. This connectivity almost certainly impacted regional climate, likely due to mixing

of waters with different temperatures and salinities. To achieve this goal, we have three specific objectives: (a) to reconstruct and combine the  $\delta^{18}\text{O}_{\text{aragonite}}$  and clumped isotope ( $\Delta_{47}$ ) temperatures of well-preserved gastropods to calculate an accurate temporal  $\delta^{18}\text{O}_{\text{water}}$  record. Clumped isotopes are based on the temperature-dependent abundance of  $^{13}\text{C}$ - $^{18}\text{O}$  bonds in  $\text{CO}_2$  within the dissolved inorganic carbon pool, a measure directly correlated to the temperature of precipitation of carbonates (Eiler, 2007). Because clumped-isotopes temperatures are not biased by changes in  $\delta^{18}\text{O}_{\text{water}}$ , they allow to disentangle water temperature from the water isotopic composition. (b) Reconstruct ostracod assemblage associations to investigate changes in paleo water-depth. (c) Determine the different hypotheses that could explain the trends observed in ostracod assemblages, clumped isotope temperatures and calculated  $\delta^{18}\text{O}_{\text{water}}$ . This includes potential relative sea-level changes, changes in continental runoff, and changes in the size of the North Sea gateway and northern component water mixing.

Our results indicate that the connection between the Atlantic Ocean and the North Sea did indeed fluctuate during the middle Eocene, with clumped isotopes highlighting changing benthic water temperatures on the continental shelf and a transient impact of the North Sea/Atlantic connection on the northern European regional climate.

The stratigraphical, micropaleontological (ostracod fauna) and geochemical data produced in our study will help to correlate the Highcliffe and Alum Bay section and improve their chronology in the future.

## 2. Materials and Methods

A ~42 m outcrop from the cliffs between Highcliffe Castle and Barton-on-Sea was described and sampled every meter (total of 34 samples, Figure 2). Lithology changes have been recognized in the field and the alphabetical subdivision A-I of Burton (1933) was applied (Figure 2). The presence of an inaccessible area prevented sampling from 2 to 10 m up section. Samples were freeze-dried, soaked in de-ionized water overnight and placed on a shaker to disaggregate them. A 63  $\mu\text{m}$  sieve was used to collect ostracods and gastropods. The picked fossil ostracods were identified under a stereomicroscope at the genus and species level, where possible. Gastropods were identified at species level. Ostracod species abundance in each sample was used to calculate diversity indexes in order to characterize the benthic paleocommunity (Harper, 1999). A constrained-based cluster analysis in Q-mode was performed to define the sequence of different biozones through time (Euclidean dissimilarity and un-weighted pair group method with arithmetic average UPGMA). The PAST software (Hammer et al., 2001), version 3.14, was used for the statistical analyses.

Gastropods from 13 samples belonging to the species *Haustator editus* were further cleaned (gentle crushing of shells, shaking and sonication for 30 min in cold  $\text{H}_2\text{O}_2$  and rinsing in ethanol) before being crushed into a fine powder using an agate mortar. The powders were used to test the preservation of the shells by determining the mineralogy with a Fourier Transform Infrared Spectroscopy (FT-IR).

Gastropod samples with preserved aragonitic compositions were then used for bulk ( $\delta^{13}\text{C}$ ,  $\delta^{18}\text{O}$ ) and clumped isotope ( $\Delta_{47}$ ). These analyses were carried out at the Stable Isotope Laboratory at Imperial College London. A minimum of three replicates analyses were made for each sample, using 3.5 mg of carbonate powder per replicate. Samples were prepared using the Imperial Batch Extraction system (IBEX Adlan et al., 2020), and measured on dual inlet Thermo MAT 253 mass spectrometers. Results were processed using the Easotope software (John & Bowen, 2016): the raw  $\Delta_{47}$  was corrected using a pressure baseline correction (Bernasconi et al., 2013), and the corrected  $\Delta_{47}$  values were reported in the I-CDES scale (Bernasconi et al., 2021) using the ETH1-4 standards and our in-house Carrara Marble (ICM) measured in the same session as the samples. The  $\Delta_{47}$  values were converted into temperature using the Anderson et al., (2021) equation. The  $\delta^{18}\text{O}_{\text{water}}$  was calculated using the formula of Kim et al. (2007). Reproducibility of the measurements is demonstrated by an average standard error of 0.01‰ for  $\Delta_{47}$ , and 0.1‰ for  $\delta^{18}\text{O}_{\text{aragonite}}$  and  $\delta^{13}\text{C}_{\text{aragonite}}$ , respectively, that is based on the long-term standard deviation of our standards and the number of sample replicates. To date, isotopic vital effects have not been identified in gastropods (Eagle et al., 2013; Henkes et al., 2013; Winkelstern et al., 2017).

## 3. Results

### 3.1. Ostracod Assemblages in the Barton Clay Formation

A total of 19 marine ostracod species belonging to 14 genera were recognized (Figures 2 and 3 and Table 1). The most abundant species is *Leguminocythereis striatopunctata*, followed by the genera *Cytheretta*, *Cytheridea* and

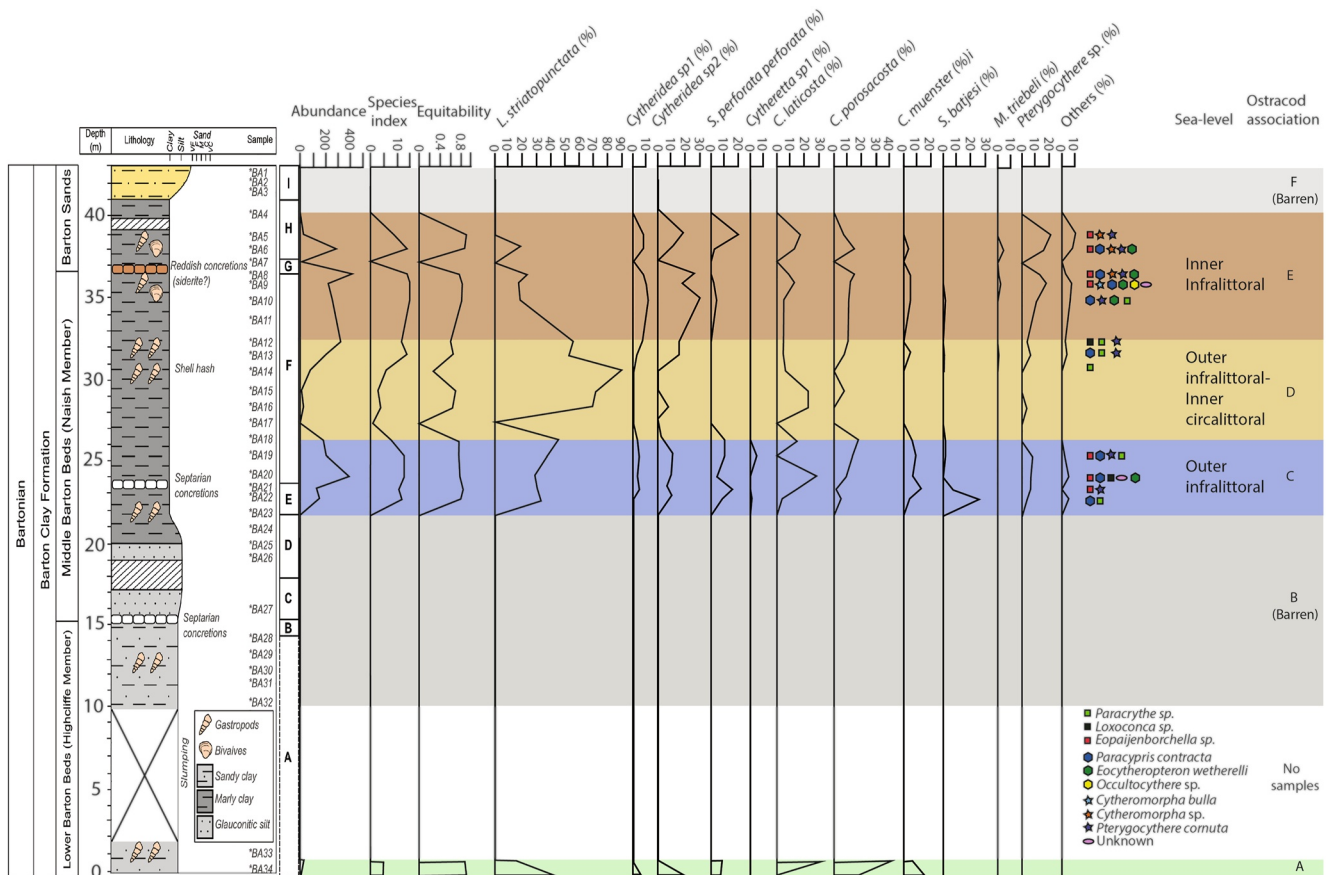


**Figure 2.** Lithology and ostracod assemblages in the Highcliffe bay section. The alphabetical subdivision A-I is referred to Burton (1933). Ostracod community index: Abundance (valves/g), Species Index (SI,  $n^{\circ}$  of species) and Equitability ( $E = H/\ln S$  where  $H$  is the Shannon index ( $H = \sum P_i \ln P_i$ , where the summation is calculated from species  $i = 1$  to species  $i = S$ ,  $P_i = n_i/n$ , and  $n$  is the total number of specimens of each  $i$  species) and  $S$  the number of species). Percentage abundances of the ostracod species recorded. “Others” include all the species present at less than 2%. They are also represented by the different symbols in the legend. The ostracod associations come from the cluster analyses and the paleo sea-level variations from the interpretation of the ecological preferences of the ostracod genera and the SI. Refer to the text for more details.

*Pterygocythere*. Four different ostracod assemblages were identified from the cluster analysis (starting from the bottom a, c, d and e), plus two barren intervals (b and f; Figure 2). Interval A includes two samples, with very few ostracods, and for this reason was considered unreliable and not further discussed. In interval C the main species are *L. striatopunctata* and *Cytheretta* followed by *Schuleridea*, *Cytheridea*, and *Cytherella*. Interval d is dominated by *L. striatopunctata* whereas *Cytheretta* and *Cytheridea* prevail in interval e. The community indexes are reported in Figure 2. Ostracod abundance and Species Index (SI) are higher in cluster c and e. Equitability is always around 0.8 indicating a good representation of each species in the assemblages.

### 3.2. Mineralogy and Sample Preservation

FT-IR analysis performed on gastropods shells used for carbonate bulk and clumped isotopes showed all samples to be pure aragonite suggesting no post-depositional alteration of the isotopic composition (Figure 4). This approach confirms the exceptional preservation of the Paleogene sequence in the Hampshire Basin.

### 3.3. Oxygen, Carbon Isotope Stratigraphy and Clumped Isotope Temperatures

The  $\delta^{18}\text{O}$  signal in the Highcliffe section is lowest in the lower part of the section (from ca. 10–20 m,  $\delta^{18}\text{O}_{\text{aragonite}} = \text{ca.} -4.0\text{‰}$ ), it increases from 20 to 25 m ( $\delta^{18}\text{O}_{\text{aragonite}}$  up to  $-2.3\text{‰}$ ) and decreases again in the uppermost part (more invariant  $\delta^{18}\text{O}_{\text{aragonite}}$  value ca.  $-3.0\text{‰}$ , Figure 5).  $\delta^{13}\text{C}_{(\text{VPDB})}$  shows a decreased trend from 1.87 to

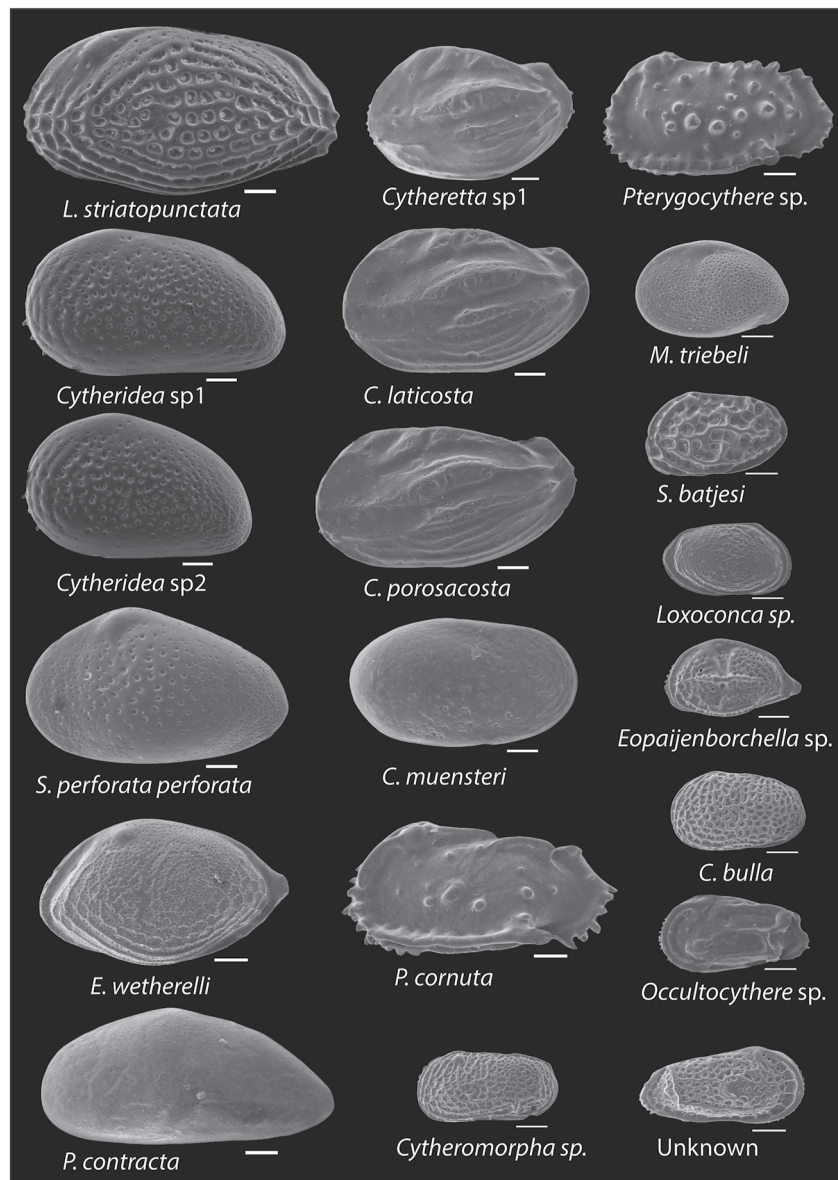


**Figure 3.** SEM pictures of the external view of selected ostracod valves. The white bars all correspond to 0.1 mm. The complete genus names of the ostracod taxa are included in Table 1.

−0.46‰ (up to 24 m), and stratigraphically above 24 m up section values become more stable with mean values around 0.9‰. An increasing trend is recorded in the uppermost part of the outcrop (Figure 5).

The  $\Delta_{47}$  values appear to be divided in two main trends: values from 0.628 to 0.592‰ (temperature range 14–25°C) mainly present in the lower part (up to 25.5 m) of the outcrops, and values from 0.590 to 0.564‰ (temperature range 26–35°C) in the upper part (Figure 5 and Table 2). This trend is even more evident in the calculated  $\delta^{18}\text{O}_{\text{water}}$  (from −2.96 to −1.77‰ and from −0.70 to 0.75‰; Figure 5 and Table 2). The  $\Delta_{47}$  and  $\delta^{18}\text{O}_{\text{water}}$  values are represented with a black point that indicates the mean value and a black line that shows two standard errors (2SE).

**Table 1**

List of the Ostracod Species Found at Highcliffe Section

Ostracod species
<i>Cytherella muensteri</i> (Roemer, 1838)
<i>Cytheretta laticosta</i> (Reuss, 1850)
<i>Cytheretta</i> sp.
<i>Cytheretta porosacosta</i> Keen, 1972
<i>Cytheridea</i> sp.1
<i>Cytheridea</i> sp.2
<i>Cytheromorpha bulla</i> Haskins, 1968
<i>Cytheromorpha</i> sp.
<i>Eocytheropteron wetherelli</i> (Jones, 1984)
<i>Eopaijenborchella</i> sp.
<i>Leguminocythereis striatopunctata</i> (Roemer)
<i>Monsmirabilia triebeli</i> Keij, 1957
<i>Occultocythereis</i> sp.
<i>Paracrythe</i> sp.
<i>Paracypris contracta</i> (Jones, 1857) Keij, 1957
<i>Pterygocythereis cornuta</i> (Roemer, 1838)
<i>Pterygocythereis</i> sp.
<i>Schizocythere batjesi</i> Keij, 1957
<i>Schuleridea perforata perforata</i> (Roemer, 1838)

## 4. Discussion

### 4.1. Water Temperature Variations

Clumped Isotope data suggest mean ocean temperatures in the Hampshire basin varied from  $\sim 14 \pm 2^\circ\text{C}$  to  $\sim 35 \pm 7^\circ\text{C}$  between  $\sim 40$  and  $41$  Ma, with mean temperatures of  $\sim 25^\circ\text{C}$ . We compare our clumped isotope temperatures ( $\Delta_{47}$ ) to temperature records from a range of localities. For optimal comparability, we only investigate records that used proxies able to provide direct measurements of temperatures (i.e.,  $\text{TEX}_{86}$  and  $\Delta_{47}$ ). During the studied interval ( $\sim 40$ – $41$  Ma) sea surface temperatures are generally stable from  $41$  to  $40.5$  with average from  $\sim 32 \pm 2.6^\circ\text{C}$  in the subtropical South Atlantic (Boscolo Galazzo et al., 2014) to  $\sim 25 \pm 2.6^\circ\text{C}$  in the Norwegian-Greenland Sea (Inglis et al., 2015, 2020) and Antarctica (Bijl et al., 2009, 2010). The trend is then interrupted by a warming event, identified as the MECO, characterized by an increase of surface temperatures from  $4$  to  $6^\circ\text{C}$  followed by a rapid decrease of global temperatures of ca.  $3^\circ\text{C}$  at its end (Bijl et al., 2009, 2010; Bohaty et al., 2009; Boscolo Galazzo et al., 2014; Cramwinckel et al., 2018, 2020; Inglis et al., 2015, 2020; Liu et al., 2009).

Because of large chronological uncertainties, it is not possible to directly compare the Highcliffe section with the aforementioned records nor to identify the exact position of the MECO event, if recorded, but we can make some observations about the general temperature trend. The Highcliffe section shows average temperatures similar to those from the Norwegian-Greenland Sea (Inglis et al., 2015, 2020; Liu et al., 2009) and Antarctica (Bijl et al., 2009, 2010), however, clumped isotopes bottom temperatures vary by as much as  $20^\circ\text{C}$  up section. This represents a greater variation in temperatures compared to the  $\text{TEX}_{86}$ -based sea surface temperatures from the Atlantic Basin ( $6^\circ\text{C}$ ; Boscolo Galazzo et al., 2014; Cramwinckel et al., 2018, 2020;

Inglis et al., 2015, 2020; Liu et al., 2009), Antarctica ( $6^\circ\text{C}$ ; Bijl et al., 2009, 2010), and the North America continental clumped isotope record ( $10^\circ\text{C}$ ; Methner et al., 2016).

The complex paleogeography of the shallow and semi-closed Hampshire basin (Figure 1) makes this site sensitive not only to the global climate changes, but also to the local variations in ocean circulation, sea-level changes and the hydrological cycle, which could in turn be triggered by the global climatic trend. The multiproxy and quantitative approach used in this study provides insights to disentangle this complex signal and to investigate the different hypotheses that could explain this extreme temperature trend.

### 4.2. Sea-Level Changes

The great abundance and good preservation of the ostracod fauna in the Barton Clay formation, first described by Haskins (1968) and by Keen (1978), allowed Keen et al. (1993) to reconstruct sea-level changes along the section based on a qualitative estimation of the ostracod species diversity (low-moderate-high diversity). In this study we improved the previous knowledge using quantitative data (species index, relative species abundance and cluster analysis) with the ecological preferences of the most abundant ostracod genera (i.e., *Leguminocythereis*, *Cytheretta*, *Cytheridea*, *Cytherella*), to reconstruct the paleo water-depth variations at Highcliffe Bay. *Leguminocythereis* is a genus that inhabits neritic environments (Şafak & Güldürek, 2016). The species *L. striatopunctata* has been designated by Ducasse and Rousselle (1985) as an indicator of the maximal phase of the marine transgression in the north Aquitaine Basin during the middle Eocene. The genus *Cytherella* can live in infra-circalittoral environments with a maximum abundance between  $70$  and  $120$  m (Bonaduce et al., 1975; Lachenal, 1989), whereas *Cytheretta* and *Cytheridea* are typical of the infralittoral area (Barbeito-González, 1971; Bonaduce et al., 1975; Breman, 1976; Lachenal, 1989). Keen et al. (1993) already observed a tight relationship between SI index and depth variations in the lower and middle Barton Clay formation (a higher species diversity corresponds to shallower environments) and recognized along the analyzed section one shallowing cycle in which the sea level decreased from  $\sim 75$  to  $0$  m. Our quantitative analyses of ostracod assemblages showed, instead, a more complex

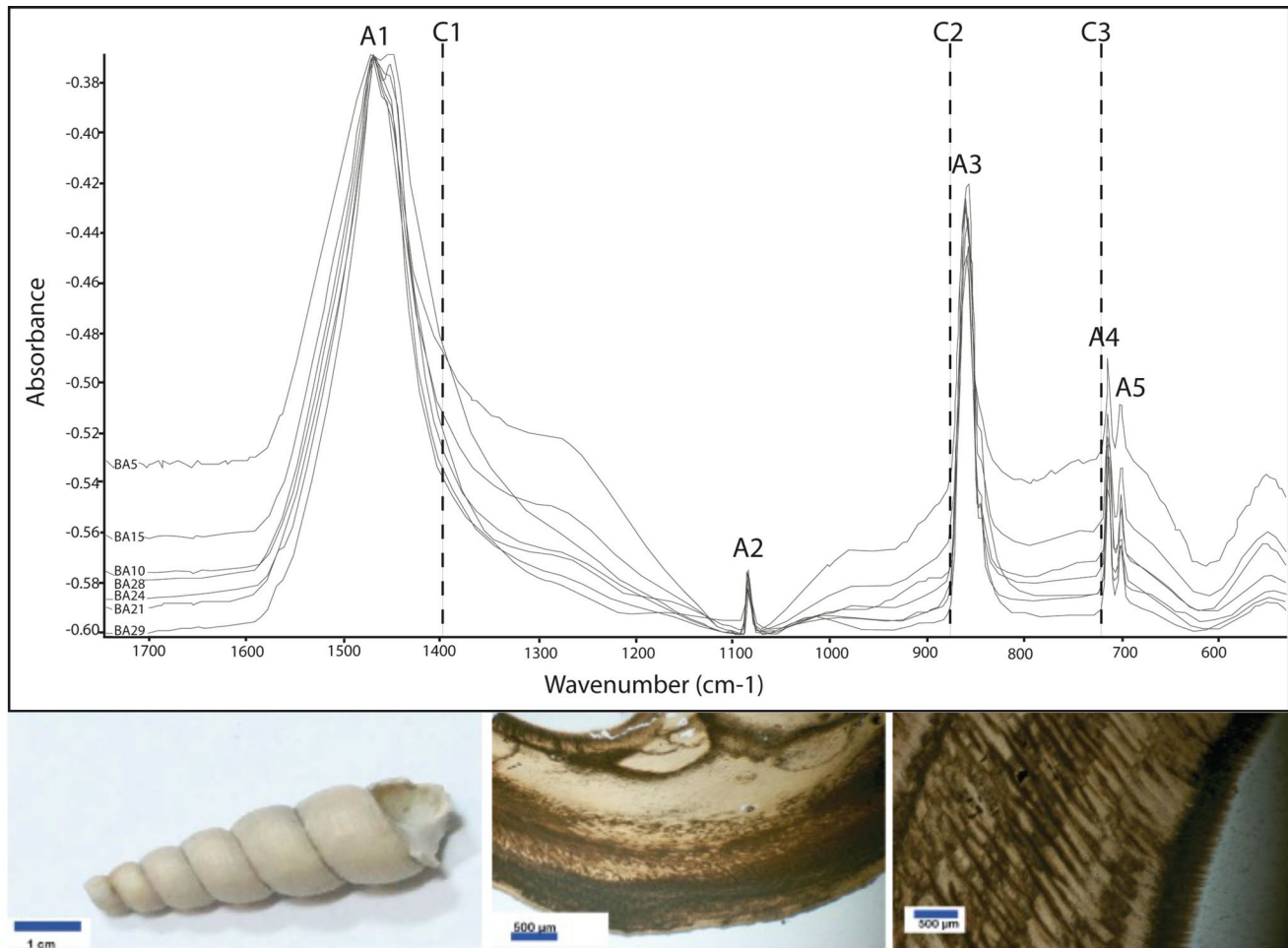


**Figure 4.** FT-IR graph of selected samples (BA5-10-15-21-24-28-29). It shows that all the gastropods' samples used for the bulk and clumped carbonate isotopes analyses are pure aragonite (A1-5). The wavenumber positions of calcite (C1-3) are indicated for comparison. The gastropods images confirm the good preservation of the shells.

environmental change: cluster c indicates an outer infralittoral environment, cluster d is interpreted as an infralittoral-inner circalittoral environment, and cluster e records a shallowing upward trend and an inner infralittoral environment (Figure 5). The maximum depth is thus of ~100 m and it is consistent with regional data obtained from benthic foraminifera at Alum Bay (Dawber et al., 2011) and the ostracod assemblages (Keen et al., 1993) at Barton-on-Sea. The sea-level variation at the Hampshire basin can be partially influenced by global changes as it matches the global eustatic curve from Miller et al. (2020) (Figure 5).

The lowest sea-level recorded corresponds in general to the highest temperatures recorded in the section (between ~30 and ~35°C) whereas the highest sea-level corresponds to the lowest temperatures (between ~14 and 25°C). In particular in the upper part of the section, from 30 to 40 m, the shallowing upward trend is accompanied by an increase in temperatures of up to  $\sim 35 \pm 7^\circ\text{C}$ . We hypothesize this might reflect the impact of sea-level changes on the local water temperatures. From thermocline model reconstructions on open Atlantic Ocean (Robinson & Stommel, 1959), it appears that paleo-water depth changes of more than 1,000 m would be needed to trigger a temperature change of 20°C. However, in shallower and semi-enclosed basins the situation appears to be more complex. The Yellow Sea, a modern shelf-sea with a maximum depth of ~150 m located between China and Korea, could be used as a modern analogue of the Hampshire basin during middle Eocene. The thermocline of the Yellow Sea shows a strong seasonality: during winter it is weaker and deeper due to the surface cooling and wind mixing, during summer it becomes shallower and stronger and a change of temperature up to ~20°C is recorded in the first 50 m (Hao et al., 2012). A recent study shows that gastropods grow more during summer

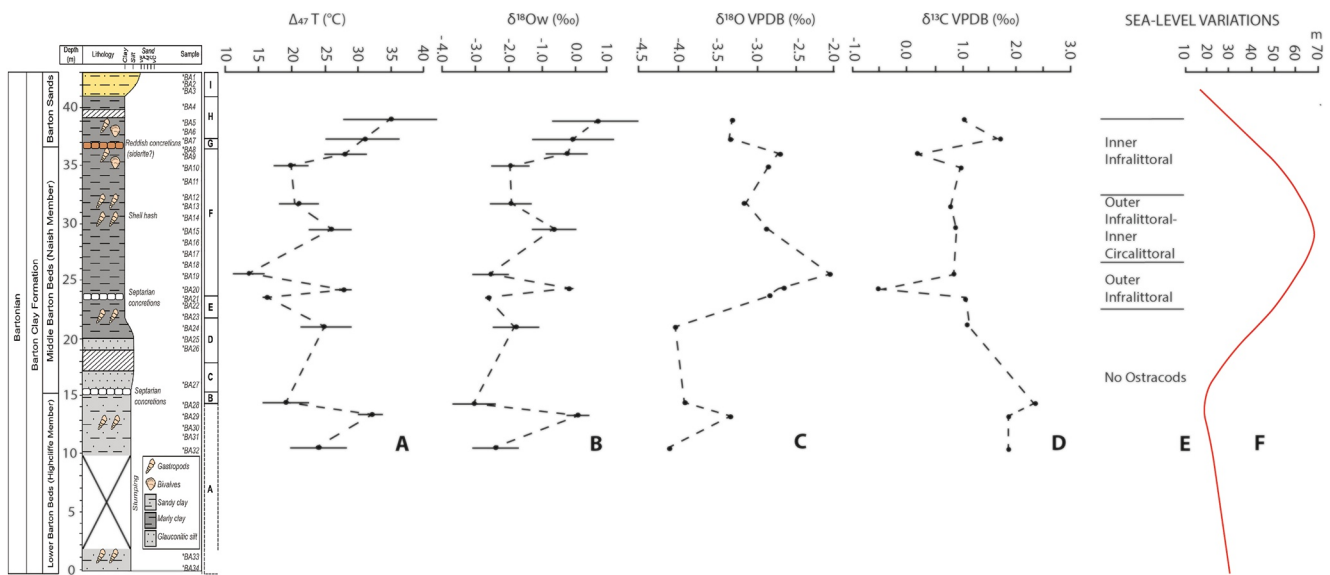


**Figure 5.** Results of geochemical analyses and sea-level variations. (a) Temperatures derived from Clumped Isotope analyses ( $\Delta_{47}$ ); (b) Isotopic water composition ( $\delta^{18}\text{O}_{\text{water}}$ ) calculated using the Kim et al. (2007) formula; (c) Bulk Oxygen ( $\delta^{18}\text{O}_{\text{aragonite}}$ ); (d) Carbon isotope ( $\delta^{13}\text{C}_{\text{aragonite}}$ ); (e) Sea-level variations reconstructed with ostracod assemblages and (f) Curve of global mean relative sea-level from Miller et al. (2020), in which the relative sea-level is expressed as the difference in height between the sea surface and the solid earth.

season and as a consequence, while reconstructing past-temperature, the colder months are less represented (De Winter et al., 2020). We speculate that inferred temperatures in the Hampshire Basin could thus reflect summer temperatures during the middle Eocene. In particular, gastropods recorded warmer temperatures (between  $\sim 30$  and  $\sim 35^\circ\text{C}$ ) above the thermocline during shallow sea-level and colder bottom temperatures (between  $\sim 14$  and  $25^\circ\text{C}$ ) below the thermocline during high sea-level intervals.

**Table 2**  
Average Carbon Isotope ( $\delta^{13}\text{C}_{\text{aragonite}}$ ) Bulk Oxygen ( $\delta^{18}\text{O}_{\text{aragonite}}$ ), Clumped Carbonate Isotope ( $\Delta_{47}$ ) and Isotopic Water ( $\delta^{18}\text{O}_{\text{water}}$ ) Composition of Each sample

ID	N <sup>o</sup>	$\delta^{13}\text{C}_{\text{aragonite}}$ (VPDB)	$\delta^{13}\text{C}_{\text{aragonite}}$ SE (VPDB)	$\delta^{18}\text{O}_{\text{aragonite}}$ (VPDB)	$\delta^{18}\text{O}_{\text{water}}$ SE (VPDB)	$\Delta_{47}$ (‰)	$\Delta_{47}$ SD (‰)	$\Delta_{47}$ SE (‰)	T (°C)	$\delta^{18}\text{O}_{\text{water}}$ (VPDB)
BA5	4	0.93	0.22	-3.27	0.03	0.564	0.04	0.02	35	0.75
BA7	3	1.5	0.51	-3.43	0.45	0.576	0.029	0.017	31	-0.12
BA9	3	0.2	0.16	-2.87	0.13	0.585	0.016	0.009	28	-0.24
BA10	3	0.88	0.09	-3.12	0.17	0.609	0.016	0.009	20	-1.97
BA13	3	1.21	0.35	-3.18	0.01	0.606	0.016	0.009	21	-2.00
BA15	4	1.01	0.09	-2.97	0.09	0.59	0.019	0.01	26	-0.70
BA19	2	1.03	0.16	-2.33	0.03	0.628	0.013	0.009	14	-2.58
BA 20	3	-0.6	0.15	-2.84	0.02	0.584	0.005	0.003	28	-0.16
BA 21	3	0.93	0.18	-2.99	0.08	0.618	0.004	0.002	17	-2.60
BA24	4	1.09	0.08	-3.67	0.09	0.592	0.021	0.01	25	-1.77
BA28	4	1.76	0.39	-3.57	0.1	0.611	0.022	0.011	19	-2.96
BA29	3	2.13	0.13	-3.51	0.11	0.573	0.011	0.006	32	0.10
BA32	4	1.75	0.13	-3.71	0.08	0.596	0.024	0.012	24	-2.12

Note. N<sup>o</sup> represents the number of replicates and the temperatures (T) are calculated using Anderson et al. (2021) equation.



### 4.3. Hydrological Cycle

Bulk isotope data from Highcliffe Bay section are very similar to those from Alum Bay in the Hampshire Basin (Dawber et al., 2011) and the Sables d'Auvers formation in the connected Paris Basin (Huyghe et al., 2015), suggesting isotopic homogeneity within the Anglo-Paris Basin. A comparison with other Eocene isotopic records (Southern Ocean: Bohaty et al., 2009; NW Atlantic Ocean: Edgar et al., 2010) reveals, instead, that on average Highcliffe Bay  $\delta^{13}\text{C}$  values are 1‰ lower than global benthic foraminifera  $\delta^{13}\text{C}$  averages. This could be explained by the higher riverine input of light carbon, in Hampshire Basin (Figure 1), which would lower the  $\delta^{13}\text{C}$  of the seawater. Compared with the Neo-Tethys restricted basin (Giorgioni et al., 2019) and the Labrador Sea (Cramwinckel et al., 2020) the Hampshire Basin values are instead very similar in  $\delta^{13}\text{C}$ . The  $\delta^{18}\text{O}$  values at Hampshire Basin are ca. 4‰ lower than global averages and 2‰ lower than restricted basins. This difference, even in similar environmental conditions, could be explained by the presence of regional effects.

Evidence of enhanced precipitations and run-off have been found during early Eocene hyperthermal events as well as in the middle Eocene during the MECO event (Carmichael et al., 2016 and reference therein). In particular, the peak-MECO event was characterized by an increase of terrigenous input, nutrient availability and low  $\delta^{18}\text{O}$  as well as reduced pedogenic carbonate concentrations that was interpreted as an intensification of the hydrological cycle (Methner et al., 2016; Rego et al., 2018; Toffanin et al., 2011; Witkowski et al., 2014). The post-MECO event is instead characterized by colder and drier climatic conditions (Bosboom et al., 2014). Eocene  $\delta^{18}\text{O}_{\text{water}}$  simulations show that, at high latitudes and mainly in closed basins the effects of  $\text{CO}_2$ -induced warming are intensified and an increase in net precipitation and freshwater flux cause a decrease of  $\delta^{18}\text{O}_{\text{water}}$  values (less saline seawaters; Zhu et al., 2020).

The  $\delta^{13}\text{C}$  negative peak associated with MECO is highly variable in terms of time and amplitude in the existing sedimentary records (Bohaty et al., 2009). For this reason, it is not possible to unambiguously interpret the  $\delta^{13}\text{C}_{\text{aragonite}}$  negative peak ( $\sim -0.46\text{‰}$ , around 24 m) in our section as the MECO event. This peak also does not correspond with the most negative  $\delta^{18}\text{O}_{\text{water}}$  values, a relationship that would have been expected if continental runoff was bringing both meteoric water and light continental carbon to the shelf. Furthermore, the most negative  $\delta^{18}\text{O}_{\text{water}}$  values correspond to lower temperatures (i.e., opposite to the expected “higher-temperature/higher run-off” model; Zhu et al., 2020). This indicates more complex feedback mechanisms in the Hampshire Basin during the middle Eocene and that the global trend and possibly the MECO event were at least partially overwritten by regional effects such as changes in local oceanic circulation, in the hydrological cycle and in sea-level. Therefore, the global recorded enhanced hydrological cycle during MECO may explain some of the trends observed but cannot be the only explanation for the recorded salinity variations.

### 4.4. Intermittent North Sea and Atlantic Ocean Connection and Water Masses Mixing

Recent numerical experiments by Zhu et al. (2020) show large  $\delta^{18}\text{O}_{\text{water}}$  variation during the Eocene. Closed basins at high latitudes, such as the paleo North Sea Basin, had  $\delta^{18}\text{O}_{\text{water}}$  values  $\sim -3\text{‰}$ . By contrast, the Atlantic Ocean had values closer to  $\sim +1\text{‰}$ . In our section two groups of  $\delta^{18}\text{O}_{\text{water}}$  values are present (from  $-2.96$  to  $-1.77\text{‰}$  and from  $-0.70$  to  $0.75\text{‰}$ ), corresponding to clumped isotope temperatures of  $\sim 14\text{--}25^\circ\text{C}$  and  $\sim 26\text{--}35^\circ\text{C}$ , respectively. We propose that our data indicates the existence of temporary connections between these two water masses, as evidenced by two lines of evidence: (a) the key position of the Hampshire Basin (Figure 1) between the Atlantic Ocean and the North Sea, and (b) changes in sea-level and the hydrologic cycle in the Hampshire basin cannot alone account for the observed trends.

During the early Paleogene, the southern part of England was part of a highly dynamic broad belt of paralic and coastal plain environment (Newell, 2014). Evidence of closure of the English Channel has been recorded before the Paleocene-Eocene Thermal Maximum and at the end of the Early Eocene Climatic Optimum (Newell, 2014; Śliwińska et al., 2019). We suggest that the closure/opening of the English Channel during the middle Eocene partially influenced the ocean temperatures and salinities recorded in the Hampshire Basin. In particular, we argue that in the lower part of the section the water temperature was mitigated by the intermittent introduction of colder North Sea water within the basin, explaining the cool and less saline waters recorded, in average comparable to the Norwegian-Greenland Sea (Inglis et al., 2015, 2020). This was reversed upward when total or partial closure of the English Channel led to an increase of regional water temperatures and salinity, probably also influenced by increased evaporation, closer to the Atlantic sites (Cramwinckel et al., 2020). A similar situation

has been described by Davis and Elliott (1957) during the deposition of the London Clay formation in the lower Eocene, when the opening of a sea gateway in the northern part of the London Sea brought cool water into the Hampshire Basin and cold-fauna specimens. A subsequent opening of a south-westwards connection with the Tethys brought then a warm current and the spread of warm-water marine organisms (Davis & Elliott, 1957).

As a mechanism for the existence of a temporary connection between the Atlantic Ocean and the North Sea we propose brief sea-level variations possibly linked to steric effects or glacio-eustasy. Relative sea-level changes are recorded in our ostracod assemblages, supporting a eustatic mechanism (Figure 2). The existence of a partially glaciated Antarctica since the middle Eocene was evidenced by Gulick et al., (2017) and the recorded sea-level variations were linked to the intermittent growth and decay of ice sheets (Miller et al., 2020). In particular, during the MECO event the global increase in temperatures might have resulted in near ice-free conditions and in a sea-level rise of around 30 m (Miller et al., 2005, 2020; Zachos et al., 2008). However, in our section, a sea level rise corresponds to lower temperatures and salinities supporting the hypothesis of the North Sea water ingression that could have mitigated the effect of MECO in the Hampshire basin. The following continuous sea-level decrease, probably linked to global decrease of temperature following the end of the MECO event, led to the complete isolation of the Hampshire Basin from the colder and less saline North Sea waters and to an increase of water temperature and salinity (Figure 5).

Previous studies based on sea-level records and the distribution of ice-rafted debris indicate the existence of short-lived Northern hemisphere glaciations since the late middle Eocene (Dawber et al., 2011; Tripathi et al., 2008). Given the large differences in temperatures as well as in the  $\delta^{18}\text{O}_{\text{water}}$  between the North Atlantic and the North Sea recorded in our study we conclude that the North Sea was most likely already connected at the time, probably through shallow gateways, with the cold and less saline Arctic Ocean waters. Our data support the presence of a small Northern Hemisphere icesheet at the time as possible source of cold and less saline water.

## 5. Conclusions

The exceptional preservation of the aragonitic gastropods and ostracod assemblages, and the key position of the Hampshire Basin, revealed a more complex relationship between the global climate and regional climate response, as demonstrated using a relatively novel proxy (clumped isotopes) on well-preserved aragonitic material. After examination of the main regional factors (i.e., sea-level changes, hydrological cycle and ocean circulation) and taking into account the global climate during the studied time frame (latest Lutetian—Bartonian, middle Eocene; ~41–40 Ma) we suggest that:

1. The possible presence of a shallow and stronger summer thermocline in the Hampshire basin could partially explain the large temperature variations linked to local sea-level changes, detected by ostracod assemblages
2. In the lower part of the section, the  $\Delta_{47}$  seawater temperatures and the calculated water salinities show a higher variability probably due to intermittent inputs of colder and less saline North Sea waters into the Hampshire Basin. This high-latitude water mixing mitigated the temperature in the Hampshire Basin, with an average recorded of ca. 20°C
3. The sea-level drop recorded in the upper part of the section, might be linked to the complete closure of the English Channel and the isolation of the Hampshire Basin, as evidenced by warmer (up to ca. 35°C) and more saline Atlantic Ocean temperatures in the Hampshire Basin
4. Connectivity of the English Channel is controlled by regional sea-level changes partially related to global climate fluctuations during middle Eocene

Our study suggests that regional climate changes were impacted by local oceanographic patterns during the middle Eocene and provides new constraints for regional models simulating middle Eocene paleoceanography. Further investigations from adjacent areas are needed to estimate the extent of the influence of the North Atlantic/North Sea connection on heat distribution and on the northern European climate. Future improvement in the chronology of the section will help to better compare the Hampshire basin with records from other locations.

## Conflict of Interest

The authors declare no conflicts of interest relevant to this study.

## Data Availability Statement

Data are available at Marchegiano, Marta; John M. Cédric, 2021, "geochemical and micropaleontological data from "Disentangling the impact of the Middle Eocene Climatic Optimum in the Hampshire Basin: new insights from carbonate clumped isotopes" M. Marchegiano and C. M. John", <https://doi.org/10.7910/DVN/N775AP>, Harvard Dataverse.

## Acknowledgments

The authors wish to express their thanks for the financial support of the Swiss National Science Foundation (P2GEP2\_181063). Annabel Dale and Fiona Middleton for the support in the sampling campaign. We thank the associate editor Laia Alegret, James Barnett and the two anonymous referees for their constructive reviews, which helped improve the manuscript.

## References

- Adlan, Q., Davies, A. J., & John, C. M. (2020). Effects of oxygen plasma ashing treatment on carbonate clumped isotopes. *Rapid Communications in Mass Spectrometry*, *34*(14). <https://doi.org/10.1002/rcm.8802>
- Anderson, N., Kelson, J. R., Kele, S., Daëron, M., Bonifacie, M., Horita, J., et al. (2021). A unified clumped isotope thermometer calibration (0.5–1100C) using carbonate-based standardization. *Geochemistry*, *48*(7). <https://doi.org/10.1029/2020GL092069>
- Barbeito-González, P. (1971). Die Ostracoden des Kuestenbereiches von Naxos (Griechenland) und ihre Lebensbereiche. *Mitteilungen Aus Dem Zoologischen Museum in Hamburg*, *67*, 255–326.
- Barnet, J. (2021). *New forest geology and fossils*. The Crowood Press.
- Barton, M., & Pearce, R. B. (2015). Landslides and stratigraphy in the coastal outcrop of the Barton Clay. *Proceedings of the Geologists' Association*, *126*(6), 731–741. <https://doi.org/10.1016/j.pgeola.2015.10.001>
- Bernasconi, S., Daëron, M., Bergmann, K. D., Bonifacie, M., & Meckler, A. N. (2021). InterCarb: A community effort to improve inter-laboratory standardization of the carbonate clumped isotope thermometer using carbonate standards. *Geochemistry*, *22*(15). <https://doi.org/10.1029/2020GC009588>
- Bernasconi, S. M., Hu, B., Wacker, U., Fiebig, J., Breitenbach, S. F. M., & Rutz, T. (2013). Background effects on Faraday collectors in gas-source mass spectrometry and implications for clumped isotope measurements: Background effects on Faraday collectors in mass spectrometry. *Rapid Communications in Mass Spectrometry*, *27*(5), 603–612. <https://doi.org/10.1002/rcm.6490>
- Bijl, P. K., Houben, A. J. P., Schouten, S., Bohaty, S. M., Sluijs, A., Reichart, G.-J., et al. (2010). Transient middle Eocene atmospheric CO<sub>2</sub> and temperature variations. *Science*, *330*(6005), 819–821. <https://doi.org/10.1126/science.1193654>
- Bijl, P. K., Schouten, S., Sluijs, A., Reichart, G.-J., Zachos, J. C., & Brinkhuis, H. (2009). Early Palaeogene temperature evolution of the southwest Pacific ocean. *Nature*, *461*(7265), 776–779. <https://doi.org/10.1038/nature08399>
- Bohaty, S. M., & Zachos, J. C. (2003). Significant Southern Ocean warming event in the late middle Eocene. *Geology*, *31*(11), 1017. <https://doi.org/10.1130/G19800.1>
- Bohaty, S. M., Zachos, J. C., Florindo, F., & Delaney, M. L. (2009). Coupled greenhouse warming and deep-sea acidification in the middle Eocene: Middle Eocene warming and CCD shoaling. *Paleoceanography*, *24*(2). <https://doi.org/10.1029/2008pa001676>
- Bonaduce, G., Ciampo, G., & Masoli, M. (1975). Distribution of Ostracoda in the Adriatic sea. *Pubblazioni Stazione Zoologica*, *40*, 1–304.
- Bosboom, R. E., Abels, H. A., Hoorn, C., van den Berg, B. C. J., Guo, Z., & Dupont-Nivet, G. (2014). Aridification in continental Asia after the middle Eocene climatic optimum (MECO). *Earth and Planetary Science Letters*, *389*, 34–42. <https://doi.org/10.1016/j.epsl.2013.12.014>
- Boscolo Galazzo, F., Thomas, E., & Giusberti, L. (2015). Benthic foraminiferal response to the middle Eocene climatic optimum (MECO) in the south-eastern Atlantic (ODP site 1263). *Palaeoecology, Palaeoclimatology, Palaeoecology*, *417*, 432–444. <https://doi.org/10.1016/j.palaeo.2014.10.004>
- Boscolo Galazzo, F., Thomas, E., Pagani, M., Warren, C., Luciani, V., & Giusberti, L. (2014). The middle Eocene climatic optimum (MECO): A multiproxy record of paleoceanographic changes in the southeast Atlantic (ODP site 1263, Walvis ridge): MECO repercussions in the SE Atlantic. *Paleoceanography*, *29*(12), 1143–1161. <https://doi.org/10.1002/2014PA002670>
- Breman, E. (1976). *The distribution of ostracodes in the bottom sediments of the Adriatic Sea*. Vrij Universiteit Amsterdam.
- Burton, E. S. J. (1933). Faunal horizons of the Barton Beds in Hampshire. *Proceedings of the Geologists' Association*, *44*, 131–167.
- Carmichael, M. J., Lunt, D. J., Huber, M., Heinemann, M., Kiehl, J., LeGrande, A., et al. (2016). A model–model and data–model comparison for the early Eocene hydrological cycle. *Climate of the Past*, *12*(2), 455–481. <https://doi.org/10.5194/cp-12-455-2016>
- Cotton, L., Rivero-Cuesta, L., Franceschetti, G., Iakovleva, A., Alegret, L., Dinarès-Turell, J., et al. (2021). Reassessing the Bartonian unit stratotype at Alum bay (Isle of Wight, UK): An integrated approach. *Newsletters on Stratigraphy*, *94*042. <https://doi.org/10.1127/nos/2020/0563>
- Cramwinckel, M. J., Coxall, H. K., Śliwińska, K. K., Polling, M., Harper, D. T., Bijl, P. K., et al. (2020). A warm, stratified, and restricted Labrador Sea across the middle Eocene and its climatic optimum. *Paleoceanography and Paleoclimatology*, *35*(10). <https://doi.org/10.1029/2020PA003932>
- Cramwinckel, M. J., Huber, M., Kocken, I. J., Agnini, C., Bijl, P. K., Bohaty, S. M., et al. (2018). Synchronous tropical and polar temperature evolution in the Eocene. *Nature*, *559*(7714), 382–386. <https://doi.org/10.1038/s41586-018-0272-2>
- Cramwinckel, M. J., van der Ploeg, R., Bijl, P. K., Peterse, F., Bohaty, S. M., Röhl, U., et al. (2019). Harmful algae and export production collapse in the equatorial Atlantic during the zenith of Middle Eocene Climatic Optimum warmth. *Geology*, *47*(3), 247–250. <https://doi.org/10.1130/G45614.1>
- Davis, A. G., & Elliott, G. F. (1957). The palaeogeography of the London clay sea. *Proceedings of the Geologists' Association*, *68*(4), 255–277. [https://doi.org/10.1016/S0016-7878\(57\)80001-7](https://doi.org/10.1016/S0016-7878(57)80001-7)
- Dawber, C. F., Tripathi, A. K., Gale, A. S., MacNiocail, C., & Hesselbo, S. P. (2011). Glacioeustasy during the middle Eocene? Insights from the stratigraphy of the Hampshire basin, UK. *Palaeoecology, Palaeoclimatology, Palaeoecology*, *300*(1–4), 84–100. <https://doi.org/10.1016/j.palaeo.2010.12.012>
- De Winter, N. J., Vellekoop, J., Clark, A. J., Stassen, P., Speijer, R. P., & Claeys, P. (2020). The giant marine gastropod *campanile giganteum* (Lamarck, 1804) as a high-resolution archive of seasonality in the Eocene greenhouse world. *Geochemistry, Geophysics, Geosystems*, *21*(4). <https://doi.org/10.1029/2019GC008794>
- Ducasse, O., & Rousselle, L. (1985). Le genre *Leguminocythereis* (ostracodes) dans le Paléogène nord-aquitain: Espèces et populations. *Histoire évolutive locale*, *31*.
- Eagle, R. A., Eiler, J. M., Tripathi, A. K., Ries, J. B., Freitas, P. S., Hiebenthal, C., et al. (2013). The influence of temperature and seawater carbonate saturation state on  $\delta^{13}\text{C}$  and  $\delta^{18}\text{O}$  bond ordering in bivalve mollusks. *Biogeosciences*, *10*(7), 4591–4606. <https://doi.org/10.5194/bg-10-4591-2013>

- Edgar, K. M., Wilson, P. A., Sexton, P. F., Gibbs, S. J., Roberts, A. P., & Norris, R. D. (2010). New biostratigraphic, magnetostratigraphic and isotopic insights into the Middle Eocene Climatic Optimum in low latitudes. *Palaeogeography, Palaeoclimatology, Palaeoecology*, 297(3–4), 670–682. <https://doi.org/10.1016/j.palaeo.2010.09.016>
- Eiler, J. M. (2007). “Clumped-isotope” geochemistry—the study of naturally-occurring, multiply-substituted isotopologues. *Earth and Planetary Science Letters*, 262(3–4), 309–327. <https://doi.org/10.1016/j.epsl.2007.08.020>
- Giorgioni, M., Jovane, L., Rego, E. S., Rodelli, D., Frontalini, F., Coccioni, R., et al. (2019). Carbon cycle instability and orbital forcing during the middle Eocene climatic optimum. *Scientific Reports*, 9(1), 9357. <https://doi.org/10.1038/s41598-019-45763-2>
- Gulick, S. P. S., Shevenell, A. E., Montelli, A., Fernandez, R., Smith, C., Warny, S., et al. (2017). Initiation and long-term instability of the East Antarctic ice sheet. *Nature*, 552(7684), 225–229. <https://doi.org/10.1038/nature25026>
- Hammer, O., Harper, D. A. T., & Ryan, P. D. (2001). *PAST: Paleontological Statistics Software Package for Education and Data Analysis* (Vol. 10).
- Harper, D. A. T., & Owen, A. W. (1999). Quantitative and morphometric methods in taxonomy. In D. A. T. Harper (Ed.), *Numerical Palaeobiology*, (pp. 1–39). John Wiley and Sons Ltd.
- Hao, J., Chen, Y., Wang, F., & Lin, P. (2012). Seasonal thermocline in the China seas and northwestern Pacific ocean: Seasonal thermocline in China seas. *Journal of Geophysical Research: Oceans*, 117(C2). <https://doi.org/10.1029/2011jc007246>
- Haskins, e.w. (1968). Tertiary Ostracoda from the Isle of Wight and Barton, Hampshire, England. *Revue de Micropaleontologie: Part I*, 1968, 10: 250–260, 2pls.; Parts II and III, 1968, II: 3–12, 2pls., 161–175, 3pls.; Part IV, 1969, 12: 149–170, 4pls.; Part V, 1970, 13: 13–29, 3 pls.; Part VI, 1971, 13: 207–221, 3pls.; Part VII, 1971, 14: 147–156.
- Henkes, G. A., Passey, B. H., Wanamaker, A. D., Grossman, E. L., Ambrose, W. G., & Carroll, M. L. (2013). Carbonate clumped isotope compositions of modern marine mollusk and brachiopod shells. *Geochimica et Cosmochimica Acta*, 106, 307–325. <https://doi.org/10.1016/j.gca.2012.12.020>
- Huyghe, D., Lartaud, F., Emmanuel, L., Merle, D., & Renard, M. (2015). Palaeogene climate evolution in the Paris Basin from oxygen stable isotope ( $\delta^{18}\text{O}$ ) compositions of marine molluscs. *Journal of the Geological Society*, 172(5), 576–587. <https://doi.org/10.1144/jgs2015-016>
- Inglis, G. N., Bragg, F., Burls, N., Evans, D., Foster, G. L., Huber, M., et al. (2020). *Global mean surface temperature and climate sensitivity of the EECO, PETM and latest Paleocene* (preprint). *Feedback and Forcing/Marine Archives/Cenozoic*. <https://doi.org/10.5194/cp-2019-167>
- Inglis, G. N., Farnsworth, A., Lunt, D., Foster, G. L., Hollis, C. J., Pagani, M., et al. (2015). Descent toward the icehouse: Eocene sea surface cooling inferred from GDGT distributions: Descent toward the icehouse. *Paleoceanography*, 30(7), 1000–1020. <https://doi.org/10.1002/2014PA002723>
- John, C. M., Bohaty, S. M., Zachos, J. C., Sluijs, A., Gibbs, S., Brinkhuis, H., & Bralower, T. J. (2008). North American continental margin records of the Paleocene-Eocene thermal maximum: Implications for global carbon and hydrological cycling: Continental margin records of the PETM. *Paleoceanography*, 23(2), n/a–n/a. <https://doi.org/10.1029/2007pa001465>
- John, C. M., & Bowen, D. (2016). Community software for challenging isotope analysis: First applications of ‘Easotope’ to clumped isotopes: Community software for challenging isotope analysis. *Rapid Communications in Mass Spectrometry*, 30(21), 2285–2300. <https://doi.org/10.1002/rcm.7720>
- Jones, C. R. (1984). On *Duringia trifurcata* Jones sp. nov. *Stereo-Atlas of Ostracod Shells*, 11 (1), 13–16.
- Jones, T. R. (1857). A monograph of the tertiary Entomostraca of England. *Monograph of the Palaeontographical Society London*, 9, 1–68.
- Keen, M. C. (1972). *Mid-Tertiary Cytheretinae of North-West Europe Bulletin British Museum*, 21 (6), 1–349.
- Keen, M. C., McKenzie, K. G., & Jones, P. J. (1993). Ostracods and late Eocene cycles of sedimentation in southern England. In *Ostracoda in the earth and Life Sciences. Proceedings of the 11th International Symposium on Ostracoda*.
- Keen, M. e. (1978). The Tertiary-Palaeogene. In R. H. Bate & E. Robinson (Eds.), (eds), *A Stratigraphical Index of British Ostracoda*, (pp.385–450). Seel House Press.
- Keij, A. J. (1957). Eocene and oligocene ostracoda of Belgium. *Mémoires de l'Institut Royal des Sciences Naturelles de Belgique*, 6(23), 1–210.
- Kim, S.-T., O’Neil, J. R., Hillaire-Marcel, C., & Mucci, A. (2007). Oxygen isotope fractionation between synthetic aragonite and water: Influence of temperature and Mg<sup>2+</sup> concentration. *Geochimica et Cosmochimica Acta*, 71(19), 4704–4715. <https://doi.org/10.1016/j.gca.2007.04.019>
- Lachenal, A. M. (1989). *Ecologie des ostracodes du domaine méditerranéen. Application au Golfe de Gabès (Tunisie Orientale). Les variations du niveau marin depuis 30.000 ans* (Vol. 108, pp. 1–239). Documents Laboratoire Géologique Lyon.
- Liu, Z., Pagani, M., Zinniker, D., DeConto, R., Huber, M., Brinkhuis, H., et al. (2009). Global cooling during the Eocene-Oligocene climate transition. *Science*, 323(5918), 1187–1190. <https://doi.org/10.1126/science.1166368>
- Methner, K., Mulch, A., Fiebig, J., Wacker, U., Gerdes, A., Graham, S. A., & Chamberlain, C. P. (2016). Rapid middle Eocene temperature change in western north America. *Earth and Planetary Science Letters*, 450, 132–139. <https://doi.org/10.1016/j.epsl.2016.05.053>
- Miller, K. G., Browning, J. V., Schmely, J. W., Kopp, R. E., Mountain, G. S., & Wright, J. D. (2020). Cenozoic sea-level and cryospheric evolution from deep-sea geochemical and continental margin records. *Scientific Advances*, 6, 1–15. <https://doi.org/10.1126/sciadv.aaz1346>
- Miller, K. G., Komazin, M. A., Browning, J. V., Wright, J. D., Mountain, G. S., Katz, M. E., et al. (2005). The phanerozoic record of global sea-level change. *Science*, 310(5752), 1293–1298. <https://doi.org/10.1126/science.1116412>
- Newell, A. J. (2014). Palaeogene rivers of southern Britain: Climatic extremes, marine influence and compressional tectonics on the southern margin of the north Sea Basin. *Proceedings of the Geologists’ Association*, 125(5–6), 578–590. <https://doi.org/10.1016/j.pgeola.2014.06.004>
- Rego, E. S., Jovane, L., Hein, J. R., Sant’Anna, L. G., Giorgioni, M., Rodelli, D., & Özcan, E. (2018). Mineralogical evidence for warm and dry climatic conditions in the Neo-Tethys (eastern Turkey) during the middle Eocene. *Palaeogeography, Palaeoclimatology, Palaeoecology*, 501, 45–57. <https://doi.org/10.1016/j.palaeo.2018.04.007>
- Reuss, A. E. (1850). Die fossilen Entomostraceen des oesterreichischen Tertiaerbeckens. *Naturwissenschaftliche Abhandlungen*, 3, 41–92.
- Rivero-Cuesta, L., Westerhold, T., Agnini, C., Dallanave, E., Wilkens, R. H., & Alegret, L. (2019). Palaeoenvironmental changes at ODP site 702 (South Atlantic): Anatomy of the middle Eocene climatic optimum. *Paleoceanography and Paleoclimatology*, 34(12), 2047–2066. <https://doi.org/10.1029/2019PA003806>
- Robinson, A. R., & Stommel, H. (1959). The oceanic thermocline and the associated thermohaline circulation. *Tellus*, 11, 295–308. <https://doi.org/10.3402/tellusa.v11i3.9317>
- Roemer, F. (1838). — Die Cytherinen des Mollasse-Gebir- ges. *Neues Jahrbuch für Mineralogie und Paläontologie*, 6, 514–519.
- Şafak, Ü., & Güldürek, M. (2016). The Ostracoda assemblage of the Eocene-Oligocene transition in northwestern Thrace: Kırklareli–Edirne area (northwestern Turkey). *Journal of African Earth Sciences*, 117, 62–85. <https://doi.org/10.1016/j.jafrearsci.2015.09.013>
- Salt, L. A., Thomas, H., Prowe, A. E. F., Borges, A. V., Bozec, Y., & de Baar, H. J. W. (2013). Variability of North Sea pH and CO<sub>2</sub> in response to North Atlantic oscillation forcing: Variability of North Sea pH and CO<sub>2</sub>. *Journal of Geophysical Research: Biogeosciences*, 118(4), 1584–1592. <https://doi.org/10.1002/2013JG002306>
- Scotese, C. R. (2016). Tutorial: PALEOMAP PaleoAtlas for GPlates and the PaleoData Plotter Program.

- Śliwińska, K. K., Thomsen, E., Schouten, S., Schoon, P. L., & Heilmann-Clausen, C. (2019). Climate- and gateway-driven cooling of late Eocene to earliest Oligocene sea surface temperatures in the north Sea Basin. *Scientific Reports*, 9(1), 4458. <https://doi.org/10.1038/s41598-019-41013-7>
- Stocker, T. F., Qin, D., Plattner, G.-K., Tignor, M. M. B., Allen, S. K., Boschung, J., et al. (2013). *Working Group I Contribution to the Fifth Assessment Report of the Intergovernmental Panel on Climate Change* (Vol. 14).
- Thomas, H., Bozec, Y., Elkalay, K., & de Baar, H. J. W. (2004). Enhanced open ocean storage of CO<sub>2</sub> from shelf sea pumping. *Science*, 304(5673), 1005–1008. <https://doi.org/10.1126/science.1095491>
- Toffanin, F., Agnini, C., Fornaciari, E., Rio, D., Giusberti, L., Luciani, V., et al. (2011). Changes in calcareous nannofossil assemblages during the middle Eocene climatic optimum: Clues from the central-western Tethys (Alano section, NE Italy). *Marine Micropaleontology*, 81(1–2), 22–31. <https://doi.org/10.1016/j.marmicro.2011.07.002>
- Tripathi, A. K., Eagle, R. A., Morton, A., Dowdeswell, J. A., Atkinson, K. L., Bahé, Y., et al. (2008). Evidence for glaciation in the northern hemisphere back to 44 Ma from ice-rafted debris in the Greenland sea. *Earth and Planetary Science Letters*, 265(1–2), 112–122. <https://doi.org/10.1016/j.epsl.2007.09.045>
- Winkelstern, I. Z., Rowe, M. P., Lohmann, K. C., Defliese, W. F., Petersen, S. V., & Brewer, A. W. (2017). Meltwater pulse recorded in Last Interglacial mollusk shells from Bermuda. *Paleoceanography*, 32(2), 132–145. <https://doi.org/10.1002/2016PA003014>
- Witkowski, J., Bohaty, S. M., Edgar, K. M., & Harwood, D. M. (2014). Rapid fluctuations in mid-latitude siliceous plankton production during the middle Eocene climatic optimum (ODP site 1051, western North Atlantic). *Marine Micropaleontology*, 106, 110–129. <https://doi.org/10.1016/j.marmicro.2014.01.001>
- Zachos, J. C., Dickens, G. R., & Zeebe, R. E. (2008). An early Cenozoic perspective on greenhouse warming and carbon-cycle dynamics. *Nature*, 451(7176), 279–283. <https://doi.org/10.1038/nature06588>
- Zhu, J., Poulsen, C. J., Otto-Bliesner, B. L., Liu, Z., Brady, E. C., & Noone, D. C. (2020). Simulation of early Eocene water isotopes using an Earth system model and its implication for past climate reconstruction. *Earth and Planetary Science Letters*, 537, 116164. <https://doi.org/10.1016/j.epsl.2020.116164>